

INTERFACE CRACK IN ORTHOTROPIC KIRCHHOFF PLATES

András Szekrényes

Budapest University of Technology and Economics, Department of Applied Mechanics
1111 Budapest, Műegyetem rkp. 5, Building MM

Abstract: *The classical laminated plate theory is applied to calculate the stresses and energy release rate function in symmetrically delaminated orthotropic plates. The governing equation system of the double-plate model consists of ten equations. As an example an orthotropic simply-supported delaminated plate subjected to a point force is analyzed. The 3D finite element model of the plate was also created. Results indicate a reasonably good agreement between analytical and numerical models.*

Keywords: *composite, plate theory, J-integral, interfacial stress.*

1. INTRODUCTION

Laminated composite plates have many industrial applications, e.g. the fields of pressure vessels, bridge and bodywork construction, aeroplanes and finally but not least ship construction can be mentioned. It is well-known, that delamination is one of the major damage modes in laminated fiber-reinforced composite materials [1]. Mechanically, the formation of cracks and delamination surfaces can be characterized by the energy based principles of fracture mechanics [2]. The energy release rate (ERR) is the basic parameter to dimensionize the structures against crack initiation and propagation. The limit value of the ERR is called the critical ERR (CERR), which can be determined using standard (or nonstandard) test methods.

Although for the mode-I, mode-II and mixed-mode I/II fractures there is a consensus to use simple beam tests, for mode-III there is not an internationally accepted test method. In general it is thought that the practical significance of mode-III fracture is little, in spite of that in the last decades the attention was subsequently focused on this fracture mode. It will be shown in this paper that the bending of delaminated plates involves significant mode-III contribution; however the mode-II and mode-III fracture take place simultaneously leading to a mixed-mode II/III problem.

2. CLASSICAL PLATE MODEL WITH FLEXIBLE JOINT

In this section we analyze elastic laminated plates with symmetric delamination. The classical laminated plate model is completed with the effect of interface deformation [1] in a mixed-mode II/III plate problem. We consider the differential plate element shown in Fig. 1, which represents the uncracked plate portion. The equilibrium of forces in the x and y directions leads to:

$$\frac{\partial N_x}{\partial x} - \frac{\partial N_{xy}}{\partial y} = \tau_{xz}, \quad -\frac{\partial N_{xy}}{\partial x} + \frac{\partial N_y}{\partial y} = \tau_{yz}, \quad (1)$$

where N_x , N_y , N_{xy} are the in-plane forces and shear force, τ_{xz} , τ_{yz} are the interfacial shear stresses. Moreover, equilibrium of bending moments about axes x and y results in:

$$\frac{\partial M_x}{\partial x} + \frac{\partial M_{xy}}{\partial y} = -\tau_{xz} \frac{t}{2}, \quad \frac{\partial M_{xy}}{\partial x} + \frac{\partial M_y}{\partial y} = -\tau_{yz} \frac{t}{2}, \quad (2)$$

where M_x, M_y, M_{xy} are the bending and twisting moments, respectively, furthermore t is the thickness (see Fig. 1.). For laminated plates the relationship between the in-plane forces and strains ($\varepsilon_x^0, \varepsilon_y^0, \gamma_{xy}^0$) can be expressed as [3]:

$$\begin{bmatrix} N_x \\ N_y \\ N_{xy} \end{bmatrix} = \begin{bmatrix} A_{11} & A_{12} & 0 \\ A_{12} & A_{22} & 0 \\ 0 & 0 & A_{66} \end{bmatrix} \begin{bmatrix} \varepsilon_x^0 \\ \varepsilon_y^0 \\ \gamma_{xy}^0 \end{bmatrix}, \quad \begin{bmatrix} \varepsilon_x^0 \\ \varepsilon_y^0 \\ \gamma_{xy}^0 \end{bmatrix} = \begin{bmatrix} a_{11} & a_{12} & 0 \\ a_{12} & a_{22} & 0 \\ 0 & 0 & a_{66} \end{bmatrix} \begin{bmatrix} N_x \\ N_y \\ N_{xy} \end{bmatrix}. \quad (3)$$

The relationship between moments and curvatures is [3]:

$$\begin{bmatrix} M_x \\ M_y \\ M_{xy} \end{bmatrix} = \begin{bmatrix} D_{11} & D_{12} & 0 \\ D_{12} & D_{22} & 0 \\ 0 & 0 & D_{66} \end{bmatrix} \begin{bmatrix} -w_{,xx} \\ -w_{,yy} \\ -2w_{,xy} \end{bmatrix}, \quad (4)$$

where $w = w(x,y)$ is the plate deflection. Moreover, in Eqs. (3)-(4) A_{ij} and D_{ij} ($i,j = 1,2,6$) are the components of the extensional and bending stiffness matrices, a_{ij} (compliance matrix) is the inverse of A_{ij} [3]:

$$\underline{\underline{A}} = \sum_{k=1}^N \underline{\underline{C}}^{(k)} (z_{k+1} - z_k), \quad \underline{\underline{D}} = \frac{1}{3} \sum_{k=1}^N \underline{\underline{C}}^{(k)} (z_{k+1}^3 - z_k^3). \quad (5)$$

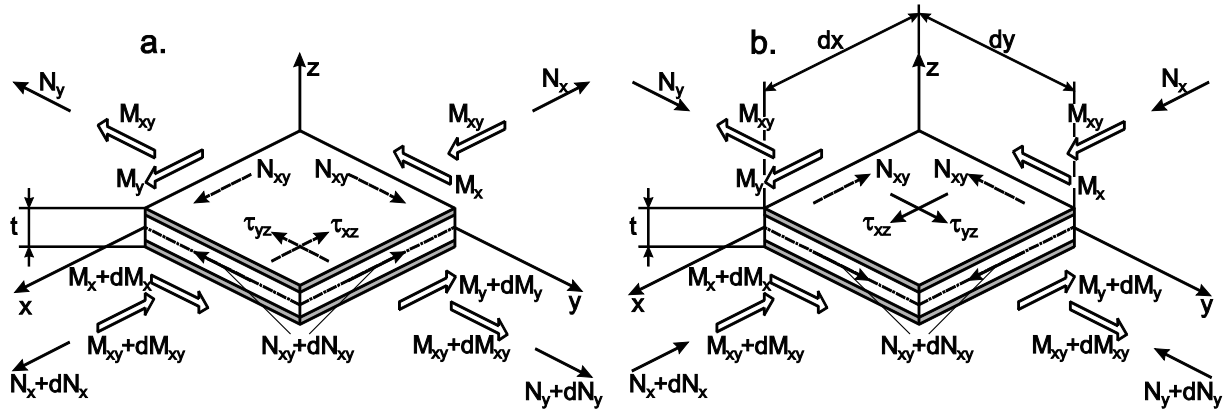


Fig.1. Equilibrium of the top (a) and bottom (b) plate elements.

The next step is the formulation of displacement continuity in the interface plane of the double-plate system. There are three different sources of in-plane displacements: in-plane normal forces, bending and shear deformation, i.e.:

$$u|_{z=-t/2} = \int (a_{11}N_x + a_{12}N_y)dx - \frac{t}{2} \frac{\partial w}{\partial x} - k_{sh}^{55} \tau_{xz} = 0, \quad (6)$$

$$v|_{z=-t/2} = \int (a_{12}N_x + a_{22}N_y)dy - \frac{t}{2} \frac{\partial w}{\partial y} - k_{sh}^{44} \tau_{yz} = 0, \quad (7)$$

where k_{sh} is the shear compliance and can be defined as the generalization of that in [1]:

$$k_{sh}^{55} = \sum_{k=1}^N \frac{z_{k+1} - z_k}{3C_{55}^{(k)}}, \quad k_{sh}^{44} = \sum_{k=1}^N \frac{z_{k+1} - z_k}{3C_{44}^{(k)}}, \quad (8)$$

where N is the number of layers, moreover the shear stiffnesses are [3]:

$$\bar{C}_{55} = C_{44} \sin^2 \theta + C_{55} \cos^2 \theta, \quad \bar{C}_{44} = C_{44} \cos^2 \theta + C_{55} \sin^2 \theta. \quad (9)$$

For plates there is a third condition formulated with respect to the in-plane shear strain:

$$\gamma_{xy}|_{z=-t/2} = -a_{66}N_{xy} - t \frac{\partial^2 w}{\partial x \partial y} - \left(k_{sh}^{55} \frac{\partial \tau_{xz}}{\partial y} + k_{sh}^{44} \frac{\partial \tau_{yz}}{\partial x} \right) = 0. \quad (10)$$

Compatibility of the displacement field requires the following:

$$\gamma_{xy}\Big|_{z=-t/2} = \frac{\partial u}{\partial y} + \frac{\partial v}{\partial x}\Big|_{z=-t/2} . \quad (11)$$

It can be seen that the second and third terms in Eqs.(6)-(7) satisfy automatically the compatibility condition. On the contrary, among the first terms the following relation can be established:

$$\frac{\partial^2 N_{xy}}{\partial x \partial y} = -\frac{1}{a_{66}} \left(a_{11} \frac{\partial^2 N_x}{\partial y^2} + a_{22} \frac{\partial^2 N_y}{\partial x^2} - a_{12} \left\{ \frac{\partial^2 N_x}{\partial x^2} + \frac{\partial^2 N_y}{\partial y^2} \right\} \right) . \quad (12)$$

Eqs. (1),(2),(4),(6),(7) and (12) define a boundary value problem including ten equations, with ten parameters: N_x , N_y , N_{xy} , τ_{xz} , τ_{yz} , M_x , M_y , M_{xy} , $\partial w/\partial x$ and $\partial w/\partial y$. Combining Eqs.(2) and (4) it is possible to derive the governing equation of the plate deflection:

$$D_{11} \frac{\partial^4 w}{\partial x^4} + 2(D_{12} + 2D_{66}) \frac{\partial^4 w}{\partial x^2 \partial y^2} + D_{22} \frac{\partial^4 w}{\partial y^4} = \frac{t}{2} \left(\frac{\partial \tau_{xz}}{\partial x} + \frac{\partial \tau_{yz}}{\partial y} \right) , \quad (13)$$

where the inhomogeneity is caused by the interface shear stresses. Also by combining the equations a PDE system can be obtained for the in-plane forces:

$$\begin{aligned} & A_1 \frac{\partial^4 N_x}{\partial x^4} + A_2 \frac{\partial^2 N_x}{\partial x^2 \partial y^2} + A_3 \frac{\partial^2 N_x}{\partial x^2} + A_4 \frac{\partial^4 N_x}{\partial y^4} + A_5 \frac{\partial^2 N_x}{\partial y^2} + \\ & + A_6 \frac{\partial^4 N_y}{\partial x^4} + A_7 \frac{\partial^2 N_y}{\partial x^2 \partial y^2} + A_8 \frac{\partial^2 N_y}{\partial x^2} + A_9 \frac{\partial^4 N_y}{\partial y^4} + A_{10} \frac{\partial^2 N_y}{\partial y^2} = 0, \end{aligned} \quad (14)$$

and similarly:

$$\begin{aligned} & B_1 \frac{\partial^4 N_y}{\partial x^4} + B_2 \frac{\partial^2 N_y}{\partial x^2 \partial y^2} + B_3 \frac{\partial^2 N_y}{\partial x^2} + B_4 \frac{\partial^4 N_y}{\partial y^4} + B_5 \frac{\partial^2 N_y}{\partial y^2} + \\ & + B_6 \frac{\partial^4 N_x}{\partial x^4} + B_7 \frac{\partial^2 N_x}{\partial x^2 \partial y^2} + B_8 \frac{\partial^2 N_x}{\partial x^2} + B_9 \frac{\partial^4 N_x}{\partial y^4} + B_{10} \frac{\partial^2 N_x}{\partial y^2} = 0, \end{aligned} \quad (15)$$

where A_i and B_i are constants depending on the stiffness and compliance parameters, as well as the thickness of the plate. Boundary conditions are necessary to solve this boundary-value problem, a specific case is presented in the next section.

3. EXAMPLE – A SIMPLY-SUPPORTED DELAMINATED PLATE

In this section we adopt Lévy plate formulation to solve the PDE system presented in section 2. Fig.2 shows a simply-supported delaminated orthotropic plate. The problem is solved in two steps: problem (a) is a traditional plate bending problem, problem (b) improves the former with the effect of crack front deformation, which was presented only for beams [1]. Here, only a brief description is given. The deflections in the cracked and uncracked part are approximated as (both for (a) and (b)):

$$w_I(x, y) = \sum_{n=1}^{\infty} W_{In}(x) \sin \beta y, \quad w_{II}(x, y) = \sum_{n=1}^{\infty} W_{II n}(x) \sin \beta y \quad (16)$$

where $\beta = n\pi/b$. The interfacial shear stresses for problem (b) are:

$$\tau_{xz}(x, y) = \sum_{n=1}^{\infty} T_n(x) \sin \beta y, \quad \tau_{yz}(x, y) = \sum_{n=1}^{\infty} R_n(x) \cos \beta y, \quad (17)$$

and finally the in-plane forces (problem (b)) can be written as:

$$N_x(x, y) = \sum_{n=1}^{\infty} n_{xn}(x) \sin \beta y, \quad N_y(x, y) = \sum_{n=1}^{\infty} n_{yn}(x) \sin \beta y, \quad N_{xy}(x, y) = \sum_{n=1}^{\infty} n_{xyn}(x) \cos \beta y . \quad (18)$$

Problem (a) can be solved in the usual way [3]. Problem (b) involves ten constants, from which eight can be determined based on the kinematic and dynamic boundary conditions with respect to the plate deflection. Further two conditions can be formulated for τ_{xz} : it vanishes at the free end ($x = -c$) and it is the highest at the delamination front. The distribution of the shear stress along the front can be obtained by the axial equilibrium of shear tractions over the midplane of the delaminated and uncracked portions [1].

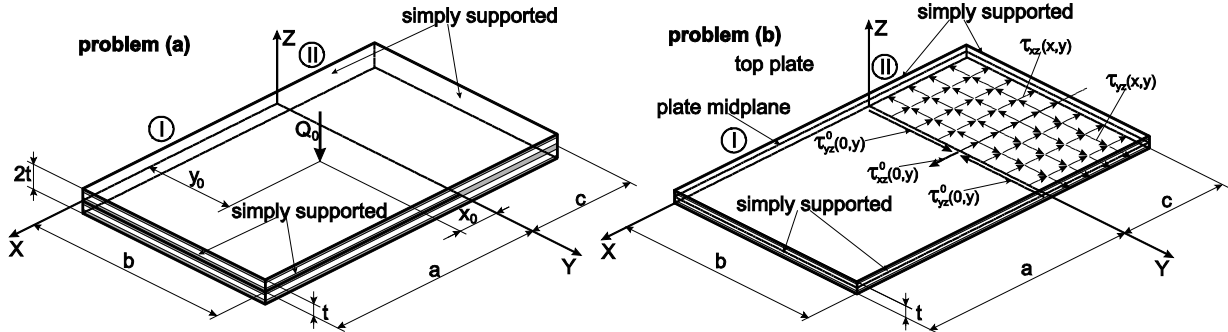


Fig. 2. A simply-supported delaminated plate subjected to a point force.

4. ENERGY RELEASE RATE – J-INTEGRAL

The energy release rate distribution over the delamination front can be calculated by the 3D J -integral [2]. The 3D J -integral is defined as [2]:

$$J_k = \int_C (Wn_k - \sigma_{ij}u_{i,k}n_j) ds + \int_A (W\delta_{k3} - \sigma_{i3}u_{i,k})_{,3} dA, \quad k=1,2, \quad J_3 = \oint_{C_c} (W_3n_1 - \sigma_{3j}u_{3,1}n_j) ds, \quad (19)$$

where n_i is the outward normal vector of the contour C , δ_{ij} is the Kronecker tensor, σ_{ij} is the stress tensor, u_i is the displacement vector, A is the area enclosed by contour C . The contour C contains the crack tip and the integration is carried out in the counterclockwise direction [2]. For the problem (a) the mode-II and mode-III integrals become:

$$J_{IIa} = -\frac{1}{2}(M_{xI}^a W_{I,xx}^a \Big|_{x=+0} - M_{xII}^a W_{II,xx}^a \Big|_{x=-0}), \quad J_{IIIa} = 2(M_{xyI}^a W_{I,xy}^a \Big|_{x=+0} - M_{xyII}^a W_{II,xy}^a \Big|_{x=-0}) \quad (20)$$

where subscript I and II refers to the delaminated and uncracked parts in Fig.2. For problem (b) we obtain (without details):

$$J_{IIb} = 2\left\{-\frac{1}{2}(M_{xI}^b W_{I,xx}^b \Big|_{x=+0} - M_{xII}^b W_{II,xx}^b \Big|_{x=-0}) + \frac{1}{2}N_x \varepsilon_x^0 \Big|_{x=-0} + \sum_{k=1}^N \int_{z_k}^{z_{k+1}} \tau_{xz}^{(k)} (w_{II,x}^b - \frac{1}{2}u_{II,z}^{b(k)}) dz \Big|_{x=-0}\right\}, \quad (21)$$

$$J_{IIIb} = 2\left\{2(M_{xyI}^b W_{I,xy}^b \Big|_{x=+0} - M_{xyII}^b W_{II,xy}^b \Big|_{x=-0}) + N_{xy} \left(\frac{1}{2}\gamma_{xy}^0 + v_{II,x}^b\right) \Big|_{x=-0} - \frac{1}{2} \sum_{k=1}^N \int_{z_k}^{z_{k+1}} \tau_{yz}^{(k)} v_{II,z}^{b(k)} dz \Big|_{x=-0}\right\}. \quad (22)$$

4. RESULTS AND DISCUSSION

The properties of the analyzed simply-supported plate were (refer to Fig. 2) the following: $a=105$ mm (crack length), $c=45$ mm (uncracked length), $b=100$ mm (plate width), $t=2$ mm (plate thickness), $Q_0=1000$ N (point force magnitude), $x_0=31$ mm, $y_0=50$ mm (point of action coordinates of Q_0). The plate is made of a carbon/epoxy material, the lay-up of the plate was $[\pm 45^{\circ f}_2; 0^{\circ}_{12}; \pm 45^{\circ f}_2]$ for the delaminated and $[\pm 45^{\circ f}_2; 0^{\circ}_{12}; \pm 45^{\circ f}_2]_S$ for the uncracked part. The superscript "f" refers to the fact that the cross-ply laminate is a woven fabric panel. The properties of the individual orthotropic laminae are $E_1=E_2=E_3=16.39$ GPa, $G_{12}=16.4$, $G_{13}=G_{23}=5.46$ GPa, $\nu_{12}=0.3$, $\nu_{13}=\nu_{23}=0.5$, for the $\pm 45^{\circ f}$ laminate and $E_1=148$ GPa, $E_2=E_3=9.65$ GPa, $G_{12}=3.71$ GPa, $G_{13}=4.66$ GPa, $G_{23}=4.91$ GPa, $\nu_{12}=0.3$, $\nu_{13}=0.25$, $\nu_{23}=0.27$, for the 0° laminate. The finite element (FE) model of the plate was also constructed, the ERR

was calculated by the virtual crack-closure technique (VCCT). Fig. 3 shows the distribution of the shear stresses [3], τ_{xz} , τ_{yz} , over the thickness at given points of the crack front, i.e. at $x=0$. It is seen that τ_{xz} changes significantly — by 42 % — compared to problem (a). Also, τ_{yz} is improved by more than twice of its original value (increase by 165 %). Thus, the shear deformation of the crack front results in significant changes in the interlaminar shear stress distributions.

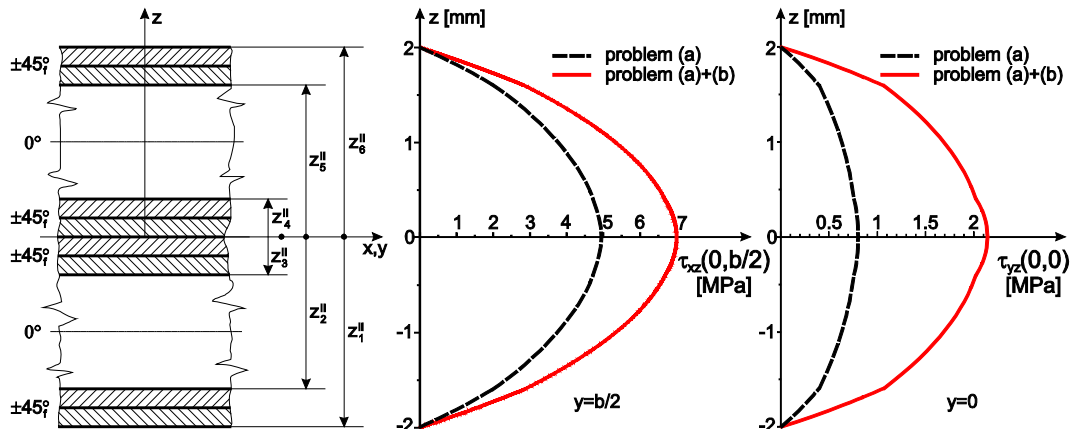


Fig. 3. Through thickness distribution of the shear stresses at certain points in the delamination front.

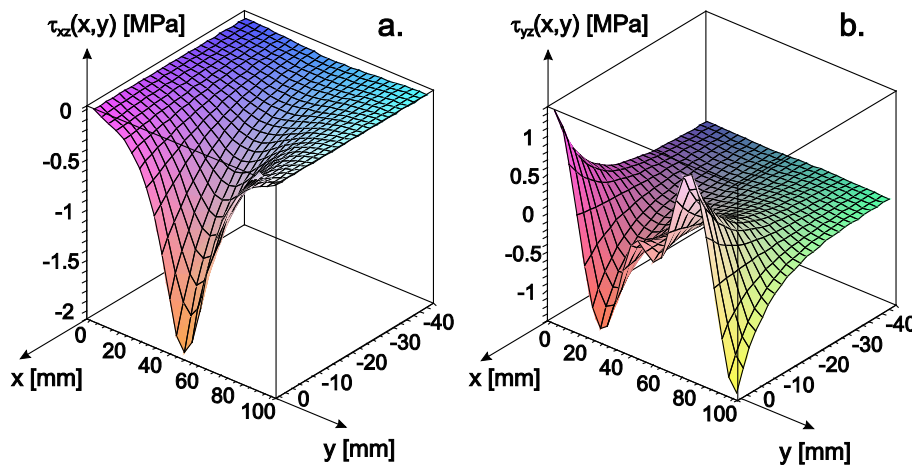


Fig. 4. Distribution of the interface shear stresses: τ_{xz} (a), τ_{yz} (b).

Fig.4 demonstrates the distribution of the shear stresses over the interface of the undelaminated region of the top plate, the stresses decay to zero behind the crack front. The mode-II, mode-III ERRs and the mode ratio along the crack front are shown by Fig.5. The symbols show the result of the VCCT [4], while the curves represent the purely analytical plate theory solutions. The solution of problem (a) provides the major part of the ERRs. It is seen that the mode-II component is significantly underestimated by the plate theory solution. On the contrary the mode-III component is overestimated. Problem (b) provides a reasonable improvement for the mode-II ERR, which is 56% for G_{II} at $y=b/2$. Also, it is clear that plate theory (a+b) underestimates the mode-II component, in the midpoint the difference is about 24% compared to the VCCT result. In contrast, the mode-III ERR is slightly smaller compared to the plate theory solution. The difference between maximum of the mode-III ERR by VCCT and the plate model is 0%, the curve crosses over the maximum point symbol.

While the VCCT predicts that the mode-III ERR decays suddenly near the edges, there is not any decay in accordance with the plate solution. In other words, edge effects are not captured properly by the plate model.

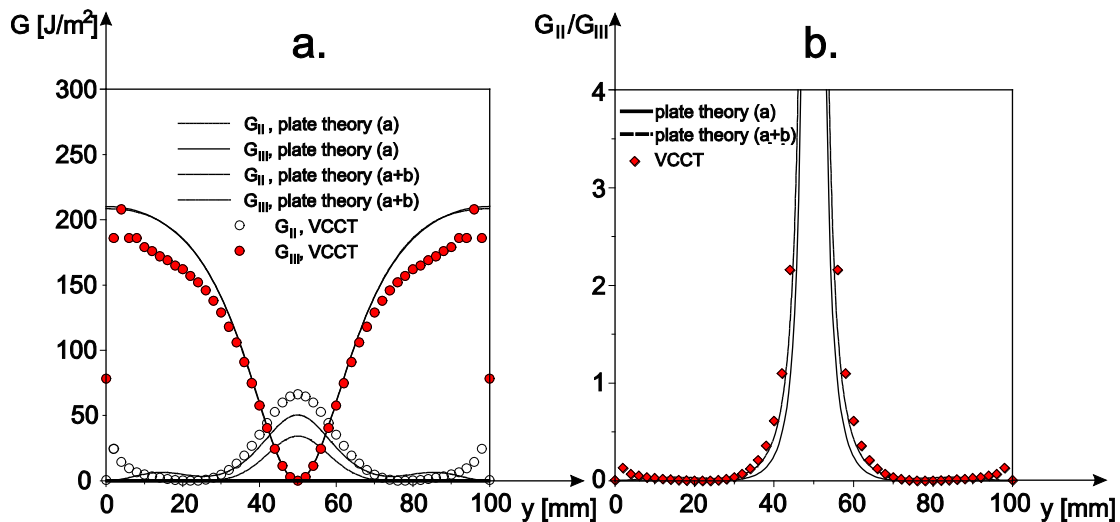


Fig. 5. Energy release rate distributions (a) and mode ratios (b) by laminated plate theory (Lévy solution) and FE analysis.

The mode ratio (G_{II}/G_{III}) is depicted in Fig.5b. The plate theory solution slightly underestimates the mode ratio, however the nature of the curves matches well with the numerical result. Also, it is clear that the improvement related to the crack front shear deformation is reasonable.

5. CONCLUSION

A purely analytical plate theory approach has been presented to calculate the shear stresses and the mode-II and mode-III ERR distributions along the crack front of symmetrically delaminated, layered composite plates subject to bending. The overall agreement between the VCCT and plate theory methods is fairly good. The difference between the VCCT and plate theory solution can be attributed to the transverse shear effect, however, it should be kept in mind that the VCCT method is also mesh sensitive.

ACKNOWLEDGMENTS

This work is connected to the scientific program of the "Development of quality-oriented and harmonized R+D+I strategy and functional model at BME" project. This project is supported by the New Hungary Development Plan (Project ID: TÁMOP-4.2.1/B-09/1/KMR-2010-0002).

REFERENCES

- [1] Wang J, Qiao P. Novel beam analysis of end notched flexure specimen for mode-II fracture. *Engineering Fracture Mechanics* 2004;71:219-231.
- [2] Rigby RH, Aliabadi MH. Decomposition of the mixed-mode J -integral - revisited. *International Journal of Solids and Structures* 1998;35(17): 2073-2099.
- [3] Reddy JN. *Mechanics of laminated composite plates and shells – Theory and Application*. Boca Raton, London, New York, Washington: CRC Press 2004.
- [4] Marat-Mendes RM, Freitas MM. Failure criteria for mixed mode delamination in glass fibre epoxy composites. *Composite Structures* 2010;92(9): 2292-2298.